

Memory Storyboard: Leveraging Temporal Segmentation for Streaming Self-Supervised Learning from Egocentric Videos

Yanlai Yang and Mengye Ren
New York University
{yy2694, mengye}@nyu.edu

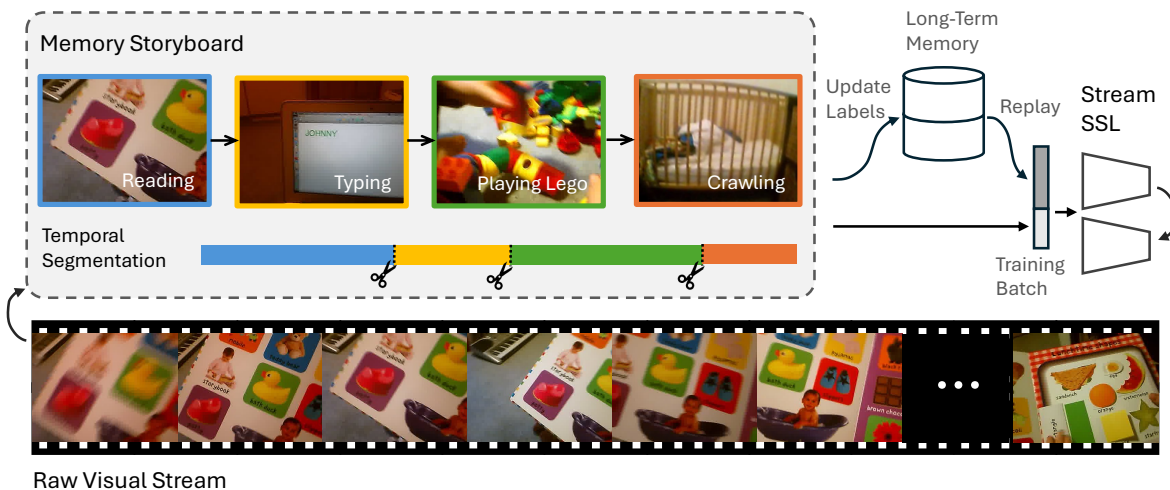


Figure 1: **Our proposed Memory Storyboard framework for streaming SSL from egocentric videos.** Similar frames are being clustered into temporal segments and their labels (text information for illustration purpose only) are updated in the long-term memory buffer for replay. SSL involves contrastive learning at both the frame and temporal segment levels.

Abstract

Self-supervised learning holds the promise to learn good representations from real-world continuous uncurated data streams. However, most existing works in visual self-supervised learning focus on static images or artificial data streams. Towards exploring a more realistic learning substrate, we investigate streaming self-supervised learning from long-form real-world egocentric video streams. Inspired by the event segmentation mechanism in human perception and memory, we propose “Memory Storyboard” that groups recent past frames into temporal segments for more effective summarization of the past visual streams for memory replay. To accommodate efficient temporal segmentation, we propose a two-tier memory hierarchy: the recent past is stored in a short-term memory, and the storyboard temporal segments are then transferred to a long-term memory. Experiments on real-world egocentric video datasets including SAYCam [55] and KrishnaCam [52] show that contrastive learning objectives on top of storyboard frames result in semantically meaningful representations which outperform those produced by state-of-the-art unsupervised continual learning methods.

1 Introduction

Humans are capable of learning continuously from a stream of unlabeled and uncurated perceptual inputs, such as video data, without needing to iterate through multiple exposures or epochs. Since early infancy, humans have accumulated knowledge about the world through a continuous flow of raw visual observations. This capability contrasts sharply with the training paradigm of current methods in self-supervised learning (SSL). While recent SSL approaches have made great strides in learning from large unlabeled datasets [11, 19, 12, 9, 7, 25, 3, 26], they still predominantly rely on static and curated image datasets, such as ImageNet [13], and needs multiple epochs of training for effective learning. This difference in paradigm raises a compelling question: how can we learn good visual representations in a streaming setting—learning from visual inputs in their original temporal order without cycling back?

Motivated by the differences of mechanisms between human learning and standard SSL, we aim to build learning algorithms that can efficiently learn visual representations and concepts from streaming video. One especially relevant mechanism in the human brain is event segmentation [37, 70], where we spontaneously segment visual streams into hierarchically structured events and identify the event boundaries. Take your recent vacation trip as an example—you probably remember separate events and activities like exploring a city, dining at a local restaurant, or relaxing at the beach. The event segmentation mechanism helps us organize memories, recall specific moments, and summarize from lengthened experiences [68, 69].

Drawing inspiration from the way we organize our memory in the brain, we introduce *Memory Storyboard*, a novel approach for streaming self-supervised learning. Memory Storyboard features a temporal segmentation module, which groups video frames into semantically meaningful temporal segments, resembling the automatic event segmentation of human cognition. Through our temporal contrastive learning objective, these temporal segments effectively facilitate representation learning in streaming videos. To accommodate efficient temporal segmentation, we propose a two-tier hierarchical memory: temporal segmentation in the short-term memory are used to update the temporal class labels in the long-term memory, and a training batch consists of samples mixed from both memories. A high-level diagram of the algorithm is shown in Figure 1.

We conduct experiments on the SAYCam [55] and KrishnaCam [52] datasets of real-world egocentric videos. Memory Storyboard outperforms state-of-the-art unsupervised continual learning methods on downstream image classification and object detection tasks, and significantly reduces the gap between streaming learning and the less flexible IID learning that requires persistent storage of the entire prior video data. We also experiment with different buffer sizes and batch sizes and offer insights on the optimal training batch composition under different memory constraints.

We summarize our contributions as follows:

- 1) We introduce Memory Storyboard, a novel streaming SSL framework that features temporal segmentation and a two-tier memory hierarchy for efficient learning and temporal abstraction.
- 2) We demonstrate that Memory Storyboard achieves state-of-the-art downstream performance when trained on real-world egocentric video datasets. Among all the streaming self-supervised learning methods we evaluated, Memory Storyboard is the only one that is competitive with or even outperforms IID training when trained on these datasets.
- 3) We study the effects of training factors including subsampling rate, average segment length, memory buffer size and training batch composition. These studies provide insight for more efficient streaming learning from videos. In particular, we explore the optimal composition ratio of the training batch from short-term vs. long-term memory, under different memory constraints. Larger batches from long-term memory improve performance when we can afford a large memory bank, while smaller batches can help prevent overfitting when we have a small memory bank.

2 Related Work

Unsupervised Continual Learning. Unsupervised Continual Learning (UCL) [44, 53] aims at learning a good representation through an unlabeled non-stationary data stream. Existing works in UCL, notably CaSSLe [17] and Osiris [73], assume that the data stream is composed of a series of episodes, and a stationary data distribution within each episode. This is not as naturalistic and human-like as our streaming setting, where the data distribution changes continuously in through the data stream, and each image appear in the

data stream only once. Meanwhile, we showed that existing UCL methods are also effective in our streaming video setting, and can be used together with the supervised contrastive objective.

Self-Supervised Learning. A large number of self-supervised representation learning methods in computer vision follows the contrastive learning framework [39, 36, 56, 26, 11, 12] which maximizes the agreement of representations of two augmented views of the same image and minimizes that of different images. Extending this idea, the supervised contrastive (SupCon) method [30] uses the labels as an extra supervision signal to get multiple positive crops for each anchor image. Other recent self-supervised learning works include pretext tasks [14, 38, 18, 41], feature space clustering [8, 9, 45], distillation with asymmetric architectures [19, 12], redundancy reduction [71, 7], and masked autoencoding [25]. Most relevant of these to our work, Orhan et al. [40] proposes the temporal classification objective, which outperforms contrastive learning objectives on the SAYCam dataset [55]. Our work enhances the temporal classification method with using a more flexible supervised contrastive objective, and leveraging temporal segmentation [42, 1], which have been used extensively in video summarization [74, 72, 48].

Streaming Learning from Videos. While a number of recent papers have studied streaming learning from images [22, 24, 23, 6], limited works have investigated the problem of streaming learning from a continuous video stream. Roady et al. [47] introduces a benchmark for streaming classification and novelty detection from videos. Zhuang et al. [75] benchmarks many self-supervised learning methods in real-time and life-long learning settings in streaming video, assuming infinite replay buffer size which is unrealistic. Most similar to our setup, Purushwalkam et al. [43] studies the task of continuous representation learning with a SimSiam objective [12] and proposes using a minimum-redundancy replay buffer. Their work also belongs to the broader range of works that study replay buffer sampling strategies in continual learning [2, 62, 57, 21]. Our work extends these prior works by adopting a two-tier replay buffer and a temporal segmentation component. Also relevant to our work, Carreira et al. [10] studies online learning from a continuous video stream with pixel-to-pixel modeling, but their exploration mainly focuses on settings without data augmentation and replay, limiting the efficacy of their framework.

Temporal Segmentation in Human Cognition. Prior research in psychology and cognitive sciences has shown that humans, including infants, are able to identify boundaries between action segments [37, 70, 5, 50, 4, 65]. Evidence in neuro-imaging further show that event segmentation is an automatic component in human perception [69]. Temporal event segmentation has proven to be critical for memory formation and retrieval [32, 16, 15, 51, 49]. The temporal segmentation component in our proposed framework is motivated by how humans interpret videos as segments with coherent semantics. We demonstrate that temporal segmentation can improve the learned visual representation.

3 Streaming SSL from Egocentric Videos

In streaming self-supervised learning, the goal is to learn useful visual representations from a continuous stream of inputs (x_1, x_2, \dots) . Here, we focus on the setting where inputs are uniformly sampled from a video stream. Similar to continual learning, we impose a memory budget so that storing the entire video would violate the constraint. Different from standard continual learning, there is no explicit notion of task, and the data distribution shift follows directly from the scene transitions of a video. The learner needs to make changes to the model as it sees new inputs, and finishes learning as soon as it receives the last input of the stream. The streaming setting is similar to Online Continual Learning [33, 20, 61], but the focus here is primarily on streaming video frames instead of a fixed dataset of static images.

Incorporating Training Batches. We use $x_{start:end}$ to denote the batch of $(end - start)$ images between x_{start} and x_{end} . At each training step t , the model fetches a new batch of b images $X_{curr} = x_{tb:(t+1)b}$ from the video stream. The model produces model updates on its parameters θ_{t+1} upon receiving X_{curr} . At the end of the video, we evaluate the final model checkpoint θ_T on various downstream tasks such as object classification and detection, which are fundamental tasks for visual scene understanding as they enable models to recognize and interpret the contents of complex environments.

Standard SSL Fails on Streaming Video. Directly applying the SSL method on X_{curr} gives very poor performance [43, 45]. This is mainly due to two reasons:

- 1) the non-stationary distribution of visual features in the stream, similar to the catastrophic forgetting problem [34] in supervised continual learning;
- 2) the high temporal correlation of images in the stream (illustrated in Figure 1). This temporal correlation breaks the IID assumption held by common optimization algorithms like SGD or Adam [31]. For contrastive learning algorithms like SimCLR [11], the similarity across different frames in the same training batch would violate the assumption that each image is different.

Memory Replay. Similar to previous works [28, 67, 43], we use a replay buffer M with finite size $|M|$ to mitigate these issues. The model can store some of the fetched images in the replay buffer, and use both samples from the replay buffer and the new frames to form a training batch of size B . By sampling from the replay buffer we de-correlate the frames in the training batch and at the same time reduce distribution shift between training batches.

4 Memory Storyboard

We present Memory Storyboard, an effective method for streaming SSL from egocentric videos. Memory Storyboard includes a temporal segmentation module and a two-tier memory hierarchy. It combines a standard self-supervised contrastive loss with a temporal contrastive objective which leverages the temporal class labels produced by the temporal segmentation module. Figure 2 illustrates the details of our method. The overall data processing and training procedure is summarized in Algorithm 2.

Temporal Segmentation. We describe our temporal segmentation algorithm as follows. Similar to Potapov et al. [42], we are given a down-sampled video frame sequence x_1, x_2, \dots, x_L , and a feature extractor f_θ . We aim to find change points t_1, t_2, \dots, t_{n-1} so that the video is divided into n semantically-consistent segments $[x_1, x_{t_1}], [x_{t_1}, x_{t_2}], \dots, [x_{t_{n-1}}, x_L]$. We also define $t_0 = 0$ and $t_n = L$. In this work, we determine the number of segments with $n = \frac{L}{T}$, where T refers to the average segment length and is a hyper-parameter.

The optimization objective of our segmentation algorithm is to maximize the average within-class similarity, i.e.

$$\max_{t_1, t_2, \dots, t_{n-1}} \sum_{i=1}^n \frac{1}{t_i - t_{i-1}} \sum_{j=t_{i-1}}^{t_i} \sum_{k=j}^{t_i} sim(x_j, x_k). \quad (1)$$

where $sim(x_j, x_k)$ denotes the cosine similarity between the embeddings $f_\theta(x_j)$ and $f_\theta(x_k)$. We compute the approximate solution to this optimization problem with a greedy approach, as detailed in Algorithm 1. We adopt this simple temporal segmentation approach in order to get good segmentation results in the beginning, when encoder network does not provide good representations. We leave it to future work for investigating different temporal segmentation strategies.

Algorithm 1 Temporal Segmentation

```
# n: number of clusters
# feats: features of the frames in the
#       sequence
# F: maximization objective (defined by
#   Equation 1).
# Returns: detected change points in the
#         stream (sorted)

def temporal_segment(n, feats, F):
    S = feats @ feats.T
    L = len(S)
    changepts = []
    for i in range(1, n):
        bestscore = 0
        for changept in range(1, L):
            temp = changepts + [changept]
            score = F(sorted(temp))
            if score > bestscore:
                bestscore = score
                bestchangept = changept
        changepts.append(bestchangept)
    return sorted(changepts)
```

Algorithm 2 Memory Storyboard Streaming SSL

```
# D: streaming data loader
# M_s: short-term memory buffer
# M_l: long-term memory buffer
# B_s, B_l: batch size for M_s, M_l
# T: default segment length
# r: subsampling rate

while True: # Loop until end of stream
    x = D.next()
    x_sub = subsample(x, r)
    M_l.add(x) # Updated with Reservoir
    M_s.add(x_sub) # Updated with FIFO
    if M_s[0].label > tc_label:
        tc_label = M_s[0].label
        n = len(M_s) / T
        feats = normalize(features(M_s))
        changes = temporal_segment(n, feats, F)
        update_labels(M_s, changes)
        update_labels(M_l, changes)
    data = sample(M_l, B_l, M_s, B_s)
    loss = TCL_loss(data) + CL_loss(data)
    model.update(loss)
```

Two-tier Memory Hierarchy. To accommodate efficient temporal segmentation, we propose a two-tier memory hierarchy. Shown in Figure 2, the system includes a long-term memory M_{long} updated with reservoir sampling [58], and a short-term memory storyboard M_{short} updated with a first-in-first-out (FIFO) strategy. We store the temporal index and the temporal class of each frame along with the image in the memory. The short-term memory size $|M_{short}|$ is much smaller than the long-term memory size $|M_{long}|$, allowing efficient temporal segmentation of the recent past. The change points produced by the temporal segmentation component on M_{short} are then used to update the temporal class labels in M_{long} .

To increase the horizon of the memory storyboard, we subsample the frames coming from the current stream before adding it to M_{short} . The subsampling also reduces the temporal correlation between the frames in the training batch sampled from M_{short} . Compared to using a single replay buffer as memory, the two-tier memory hierarchy helps avoid overfitting on the replay buffer and makes sure that the new frames are seen by the model.

Temporal Contrastive Loss. To effectively utilize the temporal class labels for representation learning, we adopt the supervised contrastive (SupCon) loss [30], which takes the samples with the same temporal class label in a batch as positives and contrasts them from the remainder of the batch. Let f_{proj} be a projector network. For a batch of images with size B , we take two random augmentations of each image to get an augmented batch $\tilde{x}_1, \tilde{x}_2, \dots, \tilde{x}_{2B}$, and compute $z_i = f_{proj}(f_\theta(\tilde{x}_j))$ be the projected features of each

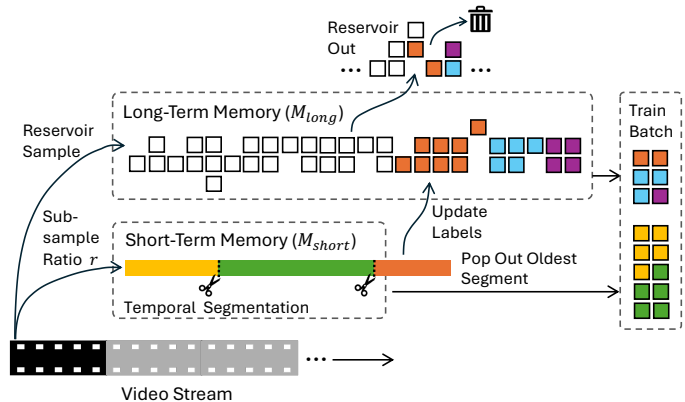


Figure 2: **Details of our two-tier memory in Memory Storyboard.** Long-term memory is updated with reservoir sampling, and short-term memory with first-in-first-out (FIFO). Temporal segmentation is applied on the short-term memory, which then updates the labels of corresponding images in the long-term memory.

Method	mini-ImageNet		ImageNet		Labeled-S		mini-ImageNet		ImageNet		Labeled-S	
	SVM	kNN	Linear	SVM	kNN	SVM	kNN	SVM	kNN	Linear	SVM	kNN
IID SimCLR [11]	44.04	34.72	30.44	59.50	59.08	44.04	34.72	30.44	59.50	59.08	44.04	34.72
IID SimSiam [12]	29.02	31.60	20.92	42.71	56.84	29.02	31.60	20.92	42.71	56.84	29.02	31.60
SimCLR No Replay	5.76	6.04	2.22	19.13	21.99	5.76	6.04	2.22	19.13	21.99	5.76	6.04
SimSiam No Replay	6.44	6.32	1.47	22.03	23.16	6.44	6.32	1.47	22.03	23.16	6.44	6.32
	<i>Replay - 10k</i>						<i>Replay - 50k</i>					
Osiris [73]	31.16	24.74	19.48	45.81	50.12	36.90	28.84	23.16	50.88	52.19	36.90	28.84
TC [40]	33.92	24.28	19.03	48.09	54.29	36.68	24.08	22.72	52.22	54.71	36.68	24.08
SimCLR [11]	33.02	26.82	20.13	49.29	53.57	37.96	30.92	23.75	53.67	56.15	37.96	30.92
+MinRed [43]	33.62	27.38	20.21	48.88	52.33	38.66	31.26	24.10	54.75	55.85	38.66	31.26
+Two-tier (Ours)	33.80	26.96	20.70	49.05	52.81	39.22	31.86	24.93	55.43	56.71	39.22	31.86
+MemStoryboard (Ours)	35.02	27.42	20.72	51.33	54.91	39.58	31.92	24.78	56.29	57.91	39.58	31.92
SimSiam [12]	20.90	27.02	13.72	39.12	54.09	26.66	30.04	14.44	43.09	56.95	26.66	30.04
+MinRed [43]	22.68	27.12	17.85	39.78	51.84	25.58	27.42	18.99	40.37	53.01	25.58	27.42
+Two-tier (Ours)	21.78	27.92	16.87	39.19	54.05	28.34	28.98	20.24	42.95	55.60	28.34	28.98
+MemStoryboard (Ours)	36.72	30.16	22.99	49.12	56.57	41.32	34.38	26.37	53.29	59.01	41.32	34.38

Table 1: **Results on streaming SSL from SAYCam [55]**. Downstream evaluation on object classification for SSL models trained under the streaming setting. For “No Replay” and “IID” the results are the same for different memory buffer sizes. The “IID” methods are not under the streaming setting and are for reference only as a performance “upper bound” with the same number of gradient updates. Unless specified, standard reservoir sampling is used in the replay buffer.

augmented image \tilde{x}_i . Let y_i be the temporal class label of \tilde{x}_i and $P(i) = \{p \in \{1, 2, \dots, 2B\} \setminus \{i\} : y_p = y_i\}$.

$$\mathcal{L}_{TCL} = \sum_i \frac{-1}{|P(i)|} \sum_{p \in P(i)} \log \frac{\exp(z_i \cdot z_p / \tau)}{\sum_{a \neq i} \exp(z_i \cdot z_a / \tau)}. \quad (2)$$

We refer to this as the temporal contrastive loss. It is conceptually similar to the temporal classification loss proposed in [40]. However, in the temporal classification loss, the size of the classification layer needs to be gradually expanded as more data is processed by the model and more temporal classes are formed. Hence the temporal contrastive loss is more flexible and more suitable for the streaming SSL setting.

Overall Loss Function. In addition to the temporal contrastive loss, we also incorporate a standard self-supervised contrastive loss \mathcal{L}_{CL} . In particular, we experimented with the SimCLR loss [11, 54] and the SimSiam loss [12] because they were shown to work well in lifelong self-supervised learning in prior works [75, 43]. The overall loss function is a sum of the temporal contrastive loss and the self-supervised contrastive loss (Equation 3).

$$\mathcal{L} = \mathcal{L}_{TCL} + \mathcal{L}_{CL}. \quad (3)$$

Warm-Start Training. At the beginning of training, the model has only seen a very limited amount of data from the video stream. Even with a memory buffer, there is likely high temporal correlation between the sampled frames and could cause instability in the training. To alleviate this problem, we warm-start the system by making no model updates on the first M_{long} frames of the stream and just use them to fill the memory. The warm-start phase ensures that the model is trained on de-correlated samples from the buffer starting from the beginning.

5 Experiments

5.1 Experiment Setup

Datasets. We use two real-world egocentric video datasets in the experiments: (1) the child S subset of SAYCam dataset [55], which contains 221 hours of video data collected from a head-mounted camera on the

Method	<i>mini</i> -ImageNet		ImageNet	OAK		<i>mini</i> -ImageNet		ImageNet	OAK	
	SVM	kNN	Linear	AP50	AP75	SVM	kNN	Linear	AP50	AP75
IID SimCLR [11]	36.90	27.54	23.77	39.54	21.84	36.90	27.54	23.77	39.54	21.84
IID SimSiam [12]	28.58	25.12	22.28	44.86	31.13	28.58	25.12	22.28	44.86	31.13
SimCLR No Replay	4.84	5.16	1.35	14.01	4.67	4.84	5.16	1.35	14.01	4.67
SimSiam No Replay	8.88	7.52	1.92	27.34	9.47	8.88	7.52	1.92	27.34	9.47
	<i>Replay - 10k</i>					<i>Replay - 50k</i>				
Osiris [73]	30.10	23.94	19.03	32.25	16.20	32.38	24.46	20.85	33.78	17.91
TC [40]	32.58	24.24	19.19	32.61	17.41	32.94	24.84	20.50	28.56	12.29
SimCLR [11]	31.46	24.70	19.09	31.92	17.40	34.98	27.14	22.37	33.30	14.92
+MinRed [43]	31.56	24.30	19.93	34.78	19.15	34.84	27.16	22.29	35.65	19.94
+Two-tier (Ours)	33.26	25.56	20.39	33.72	18.73	35.78	27.18	22.42	35.68	19.25
+MemStoryboard (Ours)	33.72	25.88	20.13	35.77	17.78	36.36	27.60	22.75	38.67	21.69
SimSiam [12]	19.16	18.84	12.94	39.38	27.31	21.84	20.18	14.13	41.13	28.62
+MinRed [43]	20.90	18.28	14.53	43.74	27.35	22.88	20.36	17.64	44.17	29.36
+Two-tier (Ours)	20.08	19.56	13.76	43.68	27.85	22.14	21.32	17.06	44.41	29.85
+MemStoryboard (Ours)	33.78	26.72	21.38	45.33	30.15	35.20	26.76	22.75	46.64	31.37

Table 2: **Results on streaming SSL from KrishnaCam [52]**. Downstream evaluation on object classification and object detection for SSL models trained on under the streaming setting. For “No Replay” and “IID” the results are the same for different memory buffer sizes. The “IID” methods are not under the streaming setting and are for reference only as a performance “upper bound” with the same number of gradient updates. Unless specified, standard reservoir sampling is used in the replay buffer.

child from age 6-32 months, decoded at 25 fps; (2) the KrishnaCam dataset [52], which contains 70 hours of video data spanning nine months of the life of a graduate student, decoded at 10 fps. These two datasets have also been adopted in a number of existing self-supervised learning literature [40, 43, 75, 59].

Training. Following the architectural choices of Osiris [73], we use ResNet-50 [27] as the feature extractor with group normalization [64] and the Mish activation function [35]. Unless otherwise specified, the default hyperparameter values we use in our experiments are $b = 64$, $B = 512$, $T = 4.5K$ for SAYCam and $T = 1.8K$ for KrishnaCam (both corresponding to 3 minutes of raw video), subsampling rate $r = 8$ for SAYCam and $r = 4$ for KrishnaCam. We train the models with two sets of memory sizes to evaluate their performance across different memory constraints: a larger memory constraint with $|M| = 50K$, $|M_{short}| = 5K$, $|M_{long}| = 45K$, and a smaller memory constraint with $|M| = 10K$, $|M_{short}| = 1K$, $|M_{long}| = 9K$. For context, there are a total of 18.2M frames in the SAYCam training set and 2.5M frame in the KrishnaCam training set. Therefore, even the large memory constraint of 50K frames only stores 0.27% and 2.01% of the total training frames in the memory buffer for SAYCam and KrishnaCam respectively.

Evaluation. For object classification, we use *mini*-ImageNet classification task for both SAYCam and KrishnaCam models. For each dataset, we also pick another downstream task that evaluates the learned representations of the training data itself. Evaluation tasks are summarized below.

- ***mini*-ImageNet classification.** Following a similar evaluation protocol as Zhuang et al. [75], we evaluate the learned representations on a downstream classification task on a subsampled ImageNet [13] dataset (*mini*-ImageNet). We extract the features of the model and train a support vector machine (SVM) or a k-nearest neighbor (kNN) classifier to measure its classification performance. The *mini*-ImageNet dataset contains 20K training images and 5K test images across 100 classes.
- **ImageNet-1K classification.** Similar to the evaluation protocol used in Purushwalkam et al. [43], we further evaluate the classification performance with a linear classifier on the larger ImageNet-1K [13] dataset with 1.28M training images and 50K test images across 1K classes.
- **Labeled-S classification.** For SAYCam models, we evaluate the classification performance on the Labeled-S dataset [40]. The the Labeled-S dataset is a labeled subset of the SAYCam frames, containing a total of 5786 images across 26 classes after 10x subsampling of frames. We randomly use 50% as training data and 50% as test data.

- **OAK object detection.** For KrishnaCam models, we evaluate the object detection performance on the Objects Around Krishna (OAK) dataset [60], which includes bounding box annotations of 105 object categories on a subset of the KrishnaCam frames. We fine-tune the model on the entire training set of OAK for 10 epochs before evaluating on the OAK validation set.

Baselines. We compare a number of competitive SSL methods for image and video representation learning, and different memory buffer strategies:

- **SimCLR.** In prior studies, Zhuang et al. [75] showed that SimCLR [11] is the strongest self-supervised learning method under streaming video setting, outperforming other SSL methods such as BYOL [19] and Barlow Twins [71].
- **SimSiam.** In prior work, Purushwalkam et al. [43] showed that SimSiam [12] is able to learn good representations from egocentric video data.
- **Osiris.** Osiris [73] is a state-of-the-art unsupervised continual learning method that is developed towards static image sequences.
- **TC.** Temporal classification (TC) [40] is a simple self-supervised learning method that is shown to work well on the SAYCam dataset under IID setting. It also uses temporal segments as a source of self-supervision; however, it does not actively group the frames together but instead relies on fixed intervals.
- **Reservoir Sampling.** We mainly use reservoir sampling [58] as a default baseline approach for updating the memory buffer, which uniformly samples from all the seen images in the memory.
- **MinRed Buffer.** The minimum redundancy (MinRed) buffer [43], also designed for the streaming setting, alleviates the temporal correlation of data in the continuous video stream by maintaining minimally redundant samples in the replay buffer.
- **Two-tier Buffer.** As in MemStoryboard, we use a long-term memory updated with reservoir sampling and short-term memory updated with first-in-first-out (FIFO), but we do not apply the temporal contrastive loss or the temporal segmentation module.

5.2 Main Results

In Tables 1 and 2, we report the main results on streaming SSL on both SAYCam and KrishnaCam. Firstly, we observe that all SSL methods work poorly in the streaming setting without replay, and larger memory leads to better performance. In terms of memory buffer strategies, our two-tier memory hierarchy and MinRed [43] outperforms reservoir sampling.

Memory Storyboard achieves superior performance in all readout tasks compared to other streaming SSL models. For SimCLR-based methods, Memory Storyboard outperforms the baseline Reservoir sampling method by an average of 1.85% on the SVM readout performance of *mini*-ImageNet classification and considerably narrows the gap between streaming learning and IID training. Memory Storyboard also significantly outperforms all baseline methods with a considerable gap by around 3% on AP50 on the challenging OAK object detection benchmark. For SimSiam-based methods, Memory Storyboard not only outperforms all streaming learning baselines by a considerable margin but also beats IID SimSiam training on all readout tasks when using a 50K replay buffer size.

Memory Storyboard with SimSiam achieves the overall best performance across different training datasets and evaluation metrics. We hypothesize that Memory Storyboard works better with SimSiam [12] than SimCLR [11] in our experiments due to the fact that SimCLR treats some highly correlated images in the same batch as negative samples during training, which hinders effective representation learning. This issue is exacerbated in the SAYCam experiments due to the high frequency (25 fps) of the SAYCam video stream. By incorporating the temporal contrastive loss in Memory Storyboard, we successfully address this issue by utilizing only images in other temporal classes as negative samples.

Overall, the results demonstrate that Memory Storyboard is effective at learning good representations from a streaming video source, and the learned representations can be successfully transferred to downstream vision tasks on the training dataset itself or an external dataset.

Qualitative Results. We visualize the temporal segments produced Memory Storyboard at the end of training in Figure 3. The results demonstrate that our temporal segmentation module can produce



Figure 3: **Visualization of the temporal segments produced by Memory Storyboard on (a) SAYCam (b)(c) KrishnaCam at the end of training.** The images are sampled at 10 seconds per frame. Each color bar correspond to a temporal class (the first and the last class might be incomplete). Temporal segments produced at the beginning of training are provided in the appendix for comparison.

semantically meaningful temporal segments, showing its strong temporal abstraction capability. We emphasize that the representations are entirely developed during the streaming SSL training as the networks are trained from scratch.

We also visualize the object detection results produced by Memory Storyboard when fine-tuned on the OAK dataset [60] in Figure 4. We observe that the fine-tuned model can successfully detect objects in cluttered environments. The results show that the representations learned by Memory Storyboard can be effectively transferred to downstream tasks which requires more fine-grained features.

5.3 Other Training Factors

In this section, we study how varying different training factors affects the performance of Memory Storyboard, including subsampling rate, average segment length, and normalization layers. For evaluation on the downstream tasks, we use SVM readout top-1 accuracy for classification tasks and AP50 for fine-tuning on OAK. We use SimCLR [11] as the base SSL method for training.

Subsampling Rate. We train Memory Storyboard with different subsampling rates when adding data fetched from the current stream to the short-term memory. Results are shown in Table 3. A subsampling ratio of 8 works best for SAYCam, while a ratio of 4 works best for KrishnaCam. Since the two datasets are decoded at different frequencies (25 fps for SAYCam and 10 fps for KrishnaCam), the effective frequency of frames entering the short-term buffer is 3.13 and 2.50 fps respectively. The result suggests that an effective frequency of around 3 fps is preferable although the optimal subsample ratio is dependent on nature of the video stream. Intuitively, when the subsampling ratio is too small, the images entering the short-term buffer may have too much temporal correlation and hence would hurt the performance; when the subsampling ratio is too big, the model skips too many frames without training on them and the temporal clustering may also



Figure 4: **Visualization of object detection results on the OAK validation set.** The Memory Storyboard model is trained on KrishnaCam and fine-tuned on the OAK training set. Red boxes show the predictions and the green boxes are ground truth bounding boxes.

become less precise.

Subsample Ratio	SAYCam		KrishnaCam	
	<i>mini</i> -ImageNet	Labeled-S	<i>mini</i> -ImageNet	OAK AP50
1×	36.70	55.29	35.54	38.55
2×	37.18	55.43	35.60	37.38
4×	38.38	55.84	36.36	38.67
8×	39.58	56.29	35.48	38.90
16×	38.62	55.81	35.88	38.22

Table 3: Effect of subsampling ratio for M_{short} in Memory Storyboard.

Average Segment Length. We trained Memory Storyboard with different average segment length T ranging from 1 minute to 10 minutes on SAYCam and KrishnaCam. The results are shown in Table 4. We demonstrate that the performance of Memory Storyboard is generally robust to average segment length (which determines the number of temporal segments in the segmentation module). We also find that the performance on downstream tasks becomes worse when the average segment length is very long ($T = 10$ min) on both datasets. This observation is different from that of temporal classification [40] which claims longer segments are more helpful.

BatchNorm vs. GroupNorm. We experimented with a variation of Memory Storyboard as well as three baseline methods (SimCLR [11], Osiris [73], and Temporal Classification [40]) where the group normalization layers in the ResNet backbone are replaced with batch normalization [29] layers. The models are trained on SAYCam and evaluated on the downstream *mini*-ImageNet classification task with a SVM. The resulting

T	SAYCam		KrishnaCam	
	<i>mini</i> -ImageNet	Labeled-S	<i>mini</i> -ImageNet	OAK AP50
1 min	38.90	55.05	35.86	38.57
2 min	39.16	56.53	36.30	38.68
3 min	39.58	56.29	36.36	38.67
5 min	39.26	56.64	36.28	38.07
10 min	38.34	55.36	35.98	37.53

Table 4: Performance of Memory Storyboard using different average temporal segment lengths.

	SimCLR	Osiris	TC	MemStoryboard
Batch Norm	33.62	33.32	33.16	33.68
Group Norm	37.96	36.90	36.68	39.58

Table 5: Group norm is better at dealing with temporal non-stationarity for streaming SSL.

accuracies are shown in Table 5. We observe that GroupNorm significantly outperform BatchNorm for all the models examined. This result is aligned the conclusion in [73] that BatchNorm is not compatible with unsupervised continual learning, and extends the conclusion to streaming SSL.

5.4 Optimal Batch Composition Under Different Memory Constraints

In Memory Storyboard, the training batch is composed of samples from both the long-term memory and the short-term memory (see Figure 2). However, the optimal composition ratio of the training batch, i.e. the optimal percentage of data in the training batch that comes from the short-term memory, is yet to be explored. Sampling more data from the short-term memory means we can digest more data within a fixed number of training steps, but there will be more distribution shift between different training batches. On the other hand, sampling more data from the long-term memory buffer may result in overfitting on the long-term memory data. In this section we experiment with different memory sizes and training composition, and demonstrate the optimal batch composition under different memory constraints.

We fix the size of the short-term memory $|M_{short}|$ to be $5K$, and vary the memory constraint for the long-term memory $|M_{long}| = 5K, 10K, 50K, 100K$. For each long-term memory size, we experiment with batch size from data stream $b = 64, 128, 192, 256, 320, 384$ (which corresponds to 12.5% though 75% of the training batch size). We sample b images from the short-term memory and $512 - b$ images from the long-term memory to compose a training batch. We evaluate the model with SVM readout on *mini*-ImageNet after the model has seen every 10% of the entire data stream and plot the results in Figure 5. We discuss the different observations for large memory size and small memory size respectively.

- **Large memory size.** When the long-term memory size is large (Figures 5(c) and 5(d)), overfitting on the memory is unlikely and hence we can sample more data from the long-term memory and the performance still keeps increasing as the model sees more data. Hence, with the same amount of data seen by the model (colored curves), it is better to sample only a small batch from the short-term memory. However, when we control the number of model update steps to the same (black curves), neither focusing on the short-term memory or focusing on the long-term memory is preferable. In such case, the optimal batch size from the short term memory is at roughly 50% of the training batch.
- **Small memory size.** When the long-term memory size is small (Figures 5(a) and 5(b)), the model is prone to overfitting on the memory. In our experiments, when at least 50% of the training batch (256 images) come from the short-term memory, the downstream task accuracy will start to decrease before we reach the end of the video stream. As a result, with the same number of model update steps (black curves), taking more images from the short-term memory gives better results. With the same amount of data seen by the model (colored curves), getting a higher percentage of long-term memory data has an advantage in the beginning when the memory size is not too small compared to the data seen by the model, but it is ultimately outperformed by models that focus more on short-term memory.

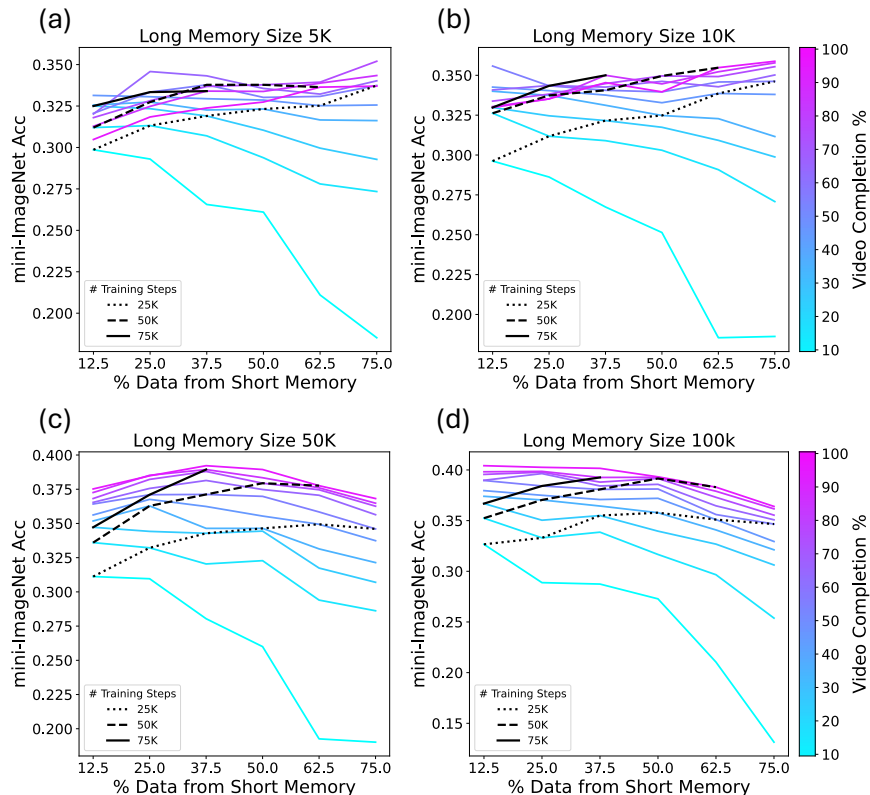


Figure 5: **Memory Storyboard model performance on SAYCam with different long-term memory sizes (5k, 10k, 50k, and 100k) and varying training batch compositions (12.5% – 75.0% from M_{short}) using SVM readout.** Each colored line represents the performance of different training batch compositions when **the model has seen the same amount of data** from the stream. Each black line represent the performance of different training batch compositions when the model has taken **the same number of gradient updates**.

To summarize, the optimal training batch composition is dependent on the memory and compute constraint. A bigger batch from the long-term memory is preferred when we can afford a relatively large memory (in our experiments, 50K images from a 200-hour video stream) and we care about the model’s performance after seeing a fixed amount of data. A smaller batch from the long-term memory is preferred when we cannot afford to a large memory to prevent overfitting on the memory buffer data. When we can afford a large memory buffer and we care about the model’s performance after a fixed amount of computation for real-time learning, a balanced training batch composition is preferred.

6 Conclusion

The ability to continuously learn from large-scale uncurated streaming video data is crucial for applying self-supervised learning methods in real-world embodied agents. Existing works have limited exploration on this problem, have mainly focused on static datasets, and do not perform well in the streaming video setting. inspired by the event segmentation mechanism in human cognition, in this work, we propose Memory Storyboard, which leverages temporal segmentation to produce a two-tier memory hierarchy akin to the short-term and long-term memory of humans. Memory Storyboard combines a temporal contrastive objective and a standard self-supervised contrastive objective to facilitate representation learning from scratch through streaming video experiences. Memory Storyboard achieves state-of-the-art performance on downstream classification and object detection tasks when trained on real-world large egocentric video datasets.

By studying the effects of subsampling rates, average segment length, normalization, and optimal batch composition under different compute and memory constraints, we also offer valuable insights on the design choices for streaming self-supervised learning.

References

- [1] Afham, M., Shukla, S. N., Poursaeed, O., Zhang, P., Shah, A., and Lim, S. (2023). Revisiting kernel temporal segmentation as an adaptive tokenizer for long-form video understanding. In *Proceedings of the IEEE/CVF International Conference on Computer Vision*, pages 1189–1194.
- [2] Aljundi, R., Lin, M., Goujaud, B., and Bengio, Y. (2019). Gradient based sample selection for online continual learning. *Advances in neural information processing systems*, 32.
- [3] Assran, M., Duval, Q., Misra, I., Bojanowski, P., Vincent, P., Rabbat, M., LeCun, Y., and Ballas, N. (2023). Self-supervised learning from images with a joint-embedding predictive architecture. In *Proceedings of the IEEE/CVF Conference on Computer Vision and Pattern Recognition*, pages 15619–15629.
- [4] Baldassano, C., Chen, J., Zadbood, A., Pillow, J. W., Hasson, U., and Norman, K. A. (2017). Discovering event structure in continuous narrative perception and memory. *Neuron*, 95(3):709–721.
- [5] Baldwin, D. A., Baird, J. A., Saylor, M. M., and Clark, M. A. (2001). Infants parse dynamic action. *Child development*, 72(3):708–717.
- [6] Banerjee, S., Verma, V. K., Parag, T., Singh, M., and Namboodiri, V. P. (2021). Class incremental online streaming learning. *arXiv preprint arXiv:2110.10741*.
- [7] Bardes, A., Ponce, J., and LeCun, Y. (2022). Vicreg: Variance-invariance-covariance regularization for self-supervised learning. In *The Tenth International Conference on Learning Representations*.
- [8] Caron, M., Bojanowski, P., Joulin, A., and Douze, M. (2018). Deep clustering for unsupervised learning of visual features. In *Proceedings of the European conference on computer vision (ECCV)*, pages 132–149.
- [9] Caron, M., Misra, I., Mairal, J., Goyal, P., Bojanowski, P., and Joulin, A. (2020). Unsupervised learning of visual features by contrasting cluster assignments. *Advances in neural information processing systems*, 33:9912–9924.
- [10] Carreira, J., King, M., Patraucean, V., Gokay, D., Ionescu, C., Yang, Y., Zoran, D., Heyward, J., Doersch, C., Aytar, Y., et al. (2024). Learning from one continuous video stream. In *Proceedings of the IEEE/CVF Conference on Computer Vision and Pattern Recognition*, pages 28751–28761.
- [11] Chen, T., Kornblith, S., Norouzi, M., and Hinton, G. (2020). A simple framework for contrastive learning of visual representations. In *International conference on machine learning*, pages 1597–1607. PMLR.
- [12] Chen, X. and He, K. (2021). Exploring simple siamese representation learning. In *Proceedings of the IEEE/CVF conference on computer vision and pattern recognition*, pages 15750–15758.
- [13] Deng, J., Dong, W., Socher, R., Li, L.-J., Li, K., and Fei-Fei, L. (2009). Imagenet: A large-scale hierarchical image database. In *2009 IEEE conference on computer vision and pattern recognition*, pages 248–255. Ieee.
- [14] Doersch, C., Gupta, A., and Efros, A. A. (2015). Unsupervised visual representation learning by context prediction. In *Proceedings of the IEEE international conference on computer vision*, pages 1422–1430.
- [15] DuBrow, S. and Davachi, L. (2013). The influence of context boundaries on memory for the sequential order of events. *Journal of Experimental Psychology: General*, 142:1277–1286.
- [16] Ezzyat, Y. and Davachi, L. (2011). What constitutes an episode in episodic memory? *Psychological science*, 22:243–52.

- [17] Fini, E., Da Costa, V. G. T., Alameda-Pineda, X., Ricci, E., Alahari, K., and Mairal, J. (2022). Self-supervised models are continual learners. In *Proceedings of the IEEE/CVF Conference on Computer Vision and Pattern Recognition*, pages 9621–9630.
- [18] Gidaris, S., Singh, P., and Komodakis, N. (2018). Unsupervised representation learning by predicting image rotations. In *6th International Conference on Learning Representations*.
- [19] Grill, J.-B., Strub, F., Altché, F., Tallec, C., Richemond, P., Buchatskaya, E., Doersch, C., Avila Pires, B., Guo, Z., Gheshlaghi Azar, M., et al. (2020). Bootstrap your own latent—a new approach to self-supervised learning. *Advances in neural information processing systems*, 33:21271–21284.
- [20] Guo, Y., Liu, B., and Zhao, D. (2022). Online continual learning through mutual information maximization. In *International conference on machine learning*, pages 8109–8126. PMLR.
- [21] Hacohen, G. and Tuytelaars, T. (2024). Forgetting order of continual learning: Examples that are learned first are forgotten last. *arXiv preprint arXiv:2406.09935*.
- [22] Hayes, T. L., Cahill, N. D., and Kanan, C. (2019). Memory efficient experience replay for streaming learning. In *2019 International Conference on Robotics and Automation (ICRA)*, pages 9769–9776. IEEE.
- [23] Hayes, T. L., Kafle, K., Shrestha, R., Acharya, M., and Kanan, C. (2020). Remind your neural network to prevent catastrophic forgetting. In *European conference on computer vision*, pages 466–483. Springer.
- [24] Hayes, T. L. and Kanan, C. (2020). Lifelong machine learning with deep streaming linear discriminant analysis. In *Proceedings of the IEEE/CVF conference on computer vision and pattern recognition workshops*, pages 220–221.
- [25] He, K., Chen, X., Xie, S., Li, Y., Dollár, P., and Girshick, R. (2022). Masked autoencoders are scalable vision learners. In *Proceedings of the IEEE/CVF conference on computer vision and pattern recognition*, pages 16000–16009.
- [26] He, K., Fan, H., Wu, Y., Xie, S., and Girshick, R. (2020). Momentum contrast for unsupervised visual representation learning. In *Proceedings of the IEEE/CVF conference on computer vision and pattern recognition*, pages 9729–9738.
- [27] He, K., Zhang, X., Ren, S., and Sun, J. (2016). Deep residual learning for image recognition. In *Proceedings of the IEEE conference on computer vision and pattern recognition*, pages 770–778.
- [28] Hu, D., Yan, S., Lu, Q., Hong, L., Hu, H., Zhang, Y., Li, Z., Wang, X., and Feng, J. (2022). How well does self-supervised pre-training perform with streaming data? In *The Tenth International Conference on Learning Representations*.
- [29] Ioffe, S. and Szegedy, C. (2015). Batch normalization: Accelerating deep network training by reducing internal covariate shift. In *Proceedings of the 32nd International Conference on Machine Learning*.
- [30] Khosla, P., Teterwak, P., Wang, C., Sarna, A., Tian, Y., Isola, P., Maschinot, A., Liu, C., and Krishnan, D. (2020). Supervised contrastive learning. *Advances in neural information processing systems*, 33:18661–18673.
- [31] Kingma, D. P. and Ba, J. (2015). Adam: A method for stochastic optimization. In *3rd International Conference on Learning Representations, ICLR 2015, San Diego, CA, USA, May 7-9, 2015, Conference Track Proceedings*.
- [32] Lassiter, G. and Slaw, D. (1991). The unitization and memory of events. *Journal of Experimental Psychology: General*, 120:80–82.
- [33] Mai, Z., Li, R., Kim, H., and Sanner, S. (2021). Supervised contrastive replay: Revisiting the nearest class mean classifier in online class-incremental continual learning. In *Proceedings of the IEEE/CVF conference on computer vision and pattern recognition*, pages 3589–3599.

- [34] McCloskey, M. and Cohen, N. J. (1989). Catastrophic interference in connectionist networks: The sequential learning problem. In *Psychology of Learning and Motivation*, volume 24, pages 109–165. Elsevier.
- [35] Misra, D. (2020). Mish: A self regularized non-monotonic activation function. In *31st British Machine Vision Conference*.
- [36] Misra, I. and Maaten, L. v. d. (2020). Self-supervised learning of pretext-invariant representations. In *Proceedings of the IEEE/CVF conference on computer vision and pattern recognition*, pages 6707–6717.
- [37] Newton, D., Engquist, G. A., and Bois, J. (1977). The objective basis of behavior units. *Journal of Personality and social psychology*, 35(12):847.
- [38] Noroozi, M. and Favaro, P. (2016). Unsupervised learning of visual representations by solving jigsaw puzzles. In *European conference on computer vision*, pages 69–84. Springer.
- [39] Oord, A. v. d., Li, Y., and Vinyals, O. (2018). Representation learning with contrastive predictive coding. *arXiv preprint arXiv:1807.03748*.
- [40] Orhan, E., Gupta, V., and Lake, B. M. (2020). Self-supervised learning through the eyes of a child. *Advances in Neural Information Processing Systems*, 33:9960–9971.
- [41] Pathak, D., Krahenbuhl, P., Donahue, J., Darrell, T., and Efros, A. A. (2016). Context encoders: Feature learning by inpainting. In *Proceedings of the IEEE conference on computer vision and pattern recognition*, pages 2536–2544.
- [42] Potapov, D., Douze, M., Harchaoui, Z., and Schmid, C. (2014). Category-specific video summarization. In *Computer Vision—ECCV 2014: 13th European Conference, Zurich, Switzerland, September 6–12, 2014, Proceedings, Part VI 13*, pages 540–555. Springer.
- [43] Purushwalkam, S., Morgado, P., and Gupta, A. (2022). The challenges of continuous self-supervised learning. In *European Conference on Computer Vision*, pages 702–721. Springer.
- [44] Rao, D., Visin, F., Rusu, A., Pascanu, R., Teh, Y. W., and Hadsell, R. (2019). Continual unsupervised representation learning. *Advances in neural information processing systems*, 32.
- [45] Ren, M., Scott, T. R., Iuzzolino, M. L., Mozer, M. C., and Zemel, R. S. (2021). Online unsupervised learning of visual representations and categories. *arXiv preprint arXiv:2109.05675*.
- [46] Ren, S., He, K., Girshick, R., and Sun, J. (2015). Faster r-cnn: Towards real-time object detection with region proposal networks. In *Advances in Neural Information Processing Systems*, volume 28.
- [47] Roady, R., Hayes, T. L., Vaidya, H., and Kanan, C. (2020). Stream-51: Streaming classification and novelty detection from videos. In *Proceedings of the IEEE/CVF Conference on Computer Vision and Pattern Recognition Workshops*, pages 228–229.
- [48] Rochan, M., Ye, L., and Wang, Y. (2018). Video summarization using fully convolutional sequence networks. In *Proceedings of the European conference on computer vision (ECCV)*, pages 347–363.
- [49] Sasmita, K. and Swallow, K. (2022). Measuring event segmentation: An investigation into the stability of event boundary agreement across groups. *Behavior Research Methods*, 55.
- [50] Saylor, M. M., Baldwin, D. A., Baird, J. A., and LaBounty, J. (2007). Infants’ on-line segmentation of dynamic human action. *Journal of Cognition and Development*, 8(1):113–128.
- [51] Silva, M., Baldassano, C., and Fuentemilla, L. (2019). Rapid memory reactivation at movie event boundaries promotes episodic encoding. *Journal of Neuroscience*, 39(43):8538–8548.
- [52] Singh, K. K., Fatahalian, K., and Efros, A. A. (2016). Krishnacam: Using a longitudinal, single-person, egocentric dataset for scene understanding tasks. In *2016 IEEE Winter Conference on Applications of Computer Vision*, pages 1–9. IEEE.

- [53] Smith, J. S., Taylor, C. E., Baer, S., and Dovrolis, C. (2021). Unsupervised progressive learning and the STAM architecture. In *Proceedings of the Thirtieth International Joint Conference on Artificial Intelligence*.
- [54] Sohn, K. (2016). Improved deep metric learning with multi-class n-pair loss objective. *Advances in neural information processing systems*, 29.
- [55] Sullivan, J., Mei, M., Perfors, A., Wojcik, E., and Frank, M. C. (2021). Saycam: A large, longitudinal audiovisual dataset recorded from the infant’s perspective. *Open mind*, 5:20–29.
- [56] Tian, Y., Krishnan, D., and Isola, P. (2020). Contrastive multiview coding. In *Computer Vision–ECCV 2020: 16th European Conference, Glasgow, UK, August 23–28, 2020, Proceedings, Part XI 16*, pages 776–794. Springer.
- [57] Tiwari, R., Killamsetty, K., Iyer, R., and Shenoy, P. (2022). Gcr: Gradient coreset based replay buffer selection for continual learning. In *Proceedings of the IEEE/CVF Conference on Computer Vision and Pattern Recognition*, pages 99–108.
- [58] Vitter, J. S. (1985). Random sampling with a reservoir. *ACM Transactions on Mathematical Software (TOMS)*, 11(1):37–57.
- [59] Vong, W. K., Wang, W., Orhan, A. E., and Lake, B. M. (2024). Grounded language acquisition through the eyes and ears of a single child. *Science*, 383(6682):504–511.
- [60] Wang, J., Wang, X., Shang-Guan, Y., and Gupta, A. (2021). Wanderlust: Online continual object detection in the real world. In *Proceedings of the IEEE/CVF international conference on computer vision*, pages 10829–10838.
- [61] Wei, Y., Ye, J., Huang, Z., Zhang, J., and Shan, H. (2023). Online prototype learning for online continual learning. In *Proceedings of the IEEE/CVF International Conference on Computer Vision*, pages 18764–18774.
- [62] Wiewel, F. and Yang, B. (2021). Entropy-based sample selection for online continual learning. In *2020 28th European signal processing conference (EUSIPCO)*, pages 1477–1481. IEEE.
- [63] Wu, J. Z., Zhang, D. J., Hsu, W., Zhang, M., and Shou, M. Z. (2023). Label-efficient online continual object detection in streaming video. In *Proceedings of the IEEE/CVF International Conference on Computer Vision*, pages 19246–19255.
- [64] Wu, Y. and He, K. (2018). Group normalization. In *Proceedings of the European conference on computer vision (ECCV)*, pages 3–19.
- [65] Yates, T. S., Skalaban, L. J., Ellis, C. T., Bracher, A. J., Baldassano, C., and Turk-Browne, N. B. (2022). Neural event segmentation of continuous experience in human infants. *Proceedings of the National Academy of Sciences*, 119(43):e2200257119.
- [66] You, Y., Gitman, I., and Ginsburg, B. (2017). Large batch training of convolutional networks. *arXiv preprint arXiv:1708.03888*.
- [67] Yu, X., Guo, Y., Gao, S., and Rosing, T. (2023). Scale: Online self-supervised lifelong learning without prior knowledge. In *Proceedings of the IEEE/CVF Conference on Computer Vision and Pattern Recognition*, pages 2484–2495.
- [68] Zacks, J. M., Speer, N. K., Vettel, J. M., and Jacoby, L. L. (2006). Event understanding and memory in healthy aging and dementia of the alzheimer type. *Psychology and aging*, 21(3):466.
- [69] Zacks, J. M. and Swallow, K. M. (2007). Event segmentation. *Current directions in psychological science*, 16(2):80–84.

- [70] Zacks, J. M., Tversky, B., and Iyer, G. (2001). Perceiving, remembering, and communicating structure in events. *Journal of experimental psychology: General*, 130(1):29.
- [71] Zbontar, J., Jing, L., Misra, I., LeCun, Y., and Deny, S. (2021). Barlow twins: Self-supervised learning via redundancy reduction. In *International conference on machine learning*, pages 12310–12320. PMLR.
- [72] Zhang, K., Chao, W.-L., Sha, F., and Grauman, K. (2016). Video summarization with long short-term memory. In *Computer Vision–ECCV 2016: 14th European Conference, Amsterdam, The Netherlands, October 11–14, 2016, Proceedings, Part VII 14*, pages 766–782. Springer.
- [73] Zhang, Y., Charlin, L., Zemel, R., and Ren, M. (2024). Integrating present and past in unsupervised continual learning. *arXiv preprint arXiv:2404.19132*.
- [74] Zhu, W., Lu, J., Li, J., and Zhou, J. (2020). Dsnet: A flexible detect-to-summarize network for video summarization. *IEEE Transactions on Image Processing*, 30:948–962.
- [75] Zhuang, C., Xiang, Z., Bai, Y., Jia, X., Turk-Browne, N., Norman, K., DiCarlo, J. J., and Yamins, D. (2022). How well do unsupervised learning algorithms model human real-time and life-long learning? *Advances in neural information processing systems*, 35:22628–22642.

A Experiment Details

Model Architecture On top of the ResNet backbone, we use a two-layer MLP with 2048 hidden units, 128 output units, and ReLU activation function as the projector. In Memory Storyboard, we create two separate projectors for \mathcal{L}_{TCL} and \mathcal{L}_{CL} .

Training For all experiments in Tables 1 and 2, we used a total batch size of 512 (64 from M_{short} and 448 from M_{long} by default). The input resolution of the images to the model is 112. We apply a standard data augmentation pipeline for SSL methods following Zhuang et al. [75], which include random resized crop, random horizontal flip, random color jitter, random gray scale, random Gaussian filter, and color-normalization with ImageNet [13]. For the SimCLR [11], Osiris [73], and TC [40] experiments, we used the Adam [31] optimizer with a constant learning rate of 0.001, and a projector with 2 MLP layers of size 2048 and 128 respectively. For the SimSiam [12] experiments, we used the SGD optimizer with learning rate 0.05, momentum 0.9, and weight decay 1e-4, and a projector with 3 MLP layers of size 2048.

Evaluation For *mini*-ImageNet and Labeled-S evaluations, the streaming SSL models are evaluated every 5% of the entire dataset. That is, we store 20 model checkpoints throughout the streaming training and evaluate them on *mini*-ImageNet and Labeled-S with SVM and kNN readout. The *best* result among these checkpoints are reported. Similar to Zhuang et al. [75], for SVM readout, we report the best performance among learning rate values {1e-7, 1e-6, 1e-5, 1e-4, 1e-3, 1e-2, 1e-1, 1, 1e1, 1e2}; for kNN readout, we report the best performance among k values {1, 3, 5, 10, 20, 50, 100, 150, 200, 250}.

For ImageNet-1K evaluations, we evaluate the final model after streaming SSL training on the entire dataset. Following Purushwalkam et al. [43], we train a linear classifier on top of the normalized learned representations and report the classification accuracy. We used the LARS [66] optimizer with learning rate 3.0, momentum 0.9, and cosine learning rate schedule for 10 epochs. We used a batch size of 1024.

For OAK evaluations, we use Faster R-CNN [46], a popular two-stage object detector. We initialize the ResNet-50 [27] backbone with the backbone of the final checkpoint of the streaming SSL model, and fine-tune the entire model on OAK with IID training for 10 epochs, following the training configurations of [63].

B Additional Results

B.1 Separating Short-term Memory Batch and Long-term Memory Batch

Inspired by the design of separating the loss on the new data and the replay data in Osiris [73], we investigate the optimal strategy of applying the temporal contrastive loss on the training batch. We consider applying

the temporal contrastive loss only on data from short-term memory, only on data from long-term memory, separately on data from short-term and long-term memory and average the losses, and on the entire training batch (concatenated data from short-term and long-term memory). We report the results in Table 6. For experiments in the main paper, we apply the temporal contrastive loss only on data from long-term memory.

The results here demonstrate that applying the temporal contrastive loss only on data from long-term memory or on the entire training batch achieve best performance. Applying the temporal contrastive loss only on data from short-term memory achieves inferior performance due to the limited number of temporal classes in the short-term buffer.

	SAYCam		KrishnaCam	
	<i>mini</i> -ImageNet	Labeled-S	<i>mini</i> -ImageNet	OAK mAP
Short Only	38.54	52.95	34.98	19.53
Long Only	39.58	56.29	36.36	21.29
Concatenate	38.34	55.43	36.08	21.20
Separate	39.42	54.95	36.70	21.40

Table 6: Performance of Memory Storyboard when the temporal contrastive loss is applied on different parts of the training batch.

C Optimal Batch Composition for SimCLR

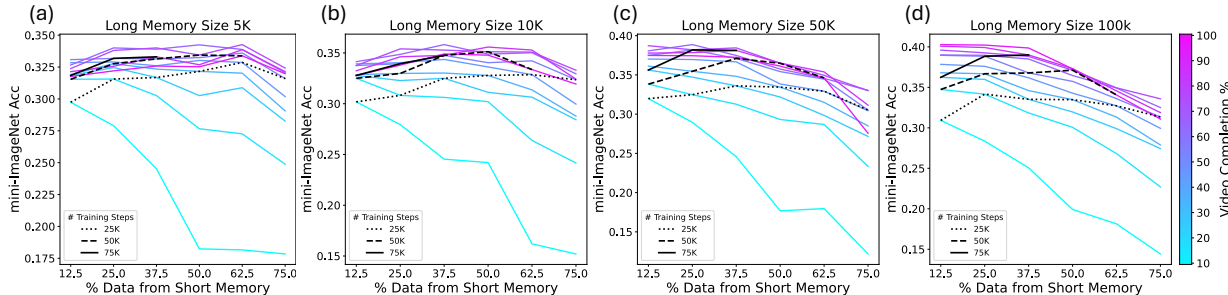


Figure 6: **SimCLR model performance on SAYCam with different long-term memory sizes (5k, 10k, 50k, and 100k) and varying training batch compositions (12.5% – 75.0% from M_{short}) using SVM readout.** Each colored line represents the performance of different training batch compositions when **the model has seen the same amount of data** from the stream. Each black line represent the performance of different training batch compositions when the model has taken **the same number of gradient updates**.

We replicate the experiments in Figure 5 on SimCLR models with two-tier memory, and plot the results in Figure 6. We observe that the analysis and the conclusions of section 5.4 still holds: when we have a large memory, we either prefer balanced training batch (with fixed amount of computation) or a bigger batch from long-term memory (with fixed amount of data); when we can only afford a small memory, we prefer a smaller batch from long-term memory. We also want to note that, the SVM readout results starts to go down towards the end of the streaming training in SimCLR experiments more often than Memory Storyboard experiments, suggesting the better scalability of Memory Storyboard to larger-scale streaming training.

These results demonstrate that the analysis and observations in section 5.4 regarding the optimal batch composition for streaming SSL training under different memory and compute constraints is general, and applies to standard SSL methods in addition to Memory Storyboard.

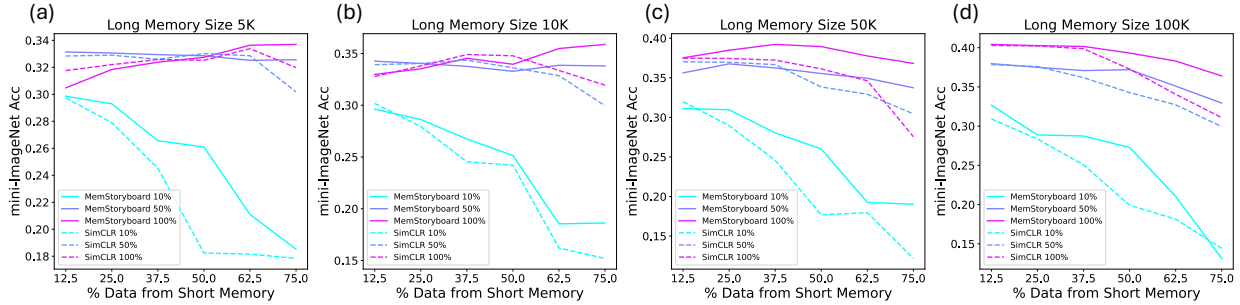


Figure 7: **Comparison of Memory Storyboard (solid lines) and SimCLR (dashed lines) model performance on SAYCam using SVM readout, controlling the amount of data the model has seen from the stream.**

D More Comprehensive Comparison between Memory Storyboard and SimCLR

With the experiment results in Figure 5 and Figure 6, we provide a more comprehensive comparison between Memory Storyboard and SimCLR performance under different memory constraints and batch compositions in Figure 7. We observe that Memory Storyboard outperforms SimCLR under the same amount of seen data, across a wide range of memory sizes and batch compositions. In particular, we note that Memory Storyboard significantly outperform SimCLR when we sample more data from M_{short} (towards the right side of the x -axis). This results in the higher optimal performance when the memory size is small, where a larger batch from M_{short} is needed to prevent overfitting on the long-term memory for better performance. We argue that, with temporal segmentation and the temporal contrastive loss, Memory Storyboard is able to provide better memory efficiency and also alleviate the temporal correlation issue suffered by SimCLR when we sample a large batch from the short-term memory.

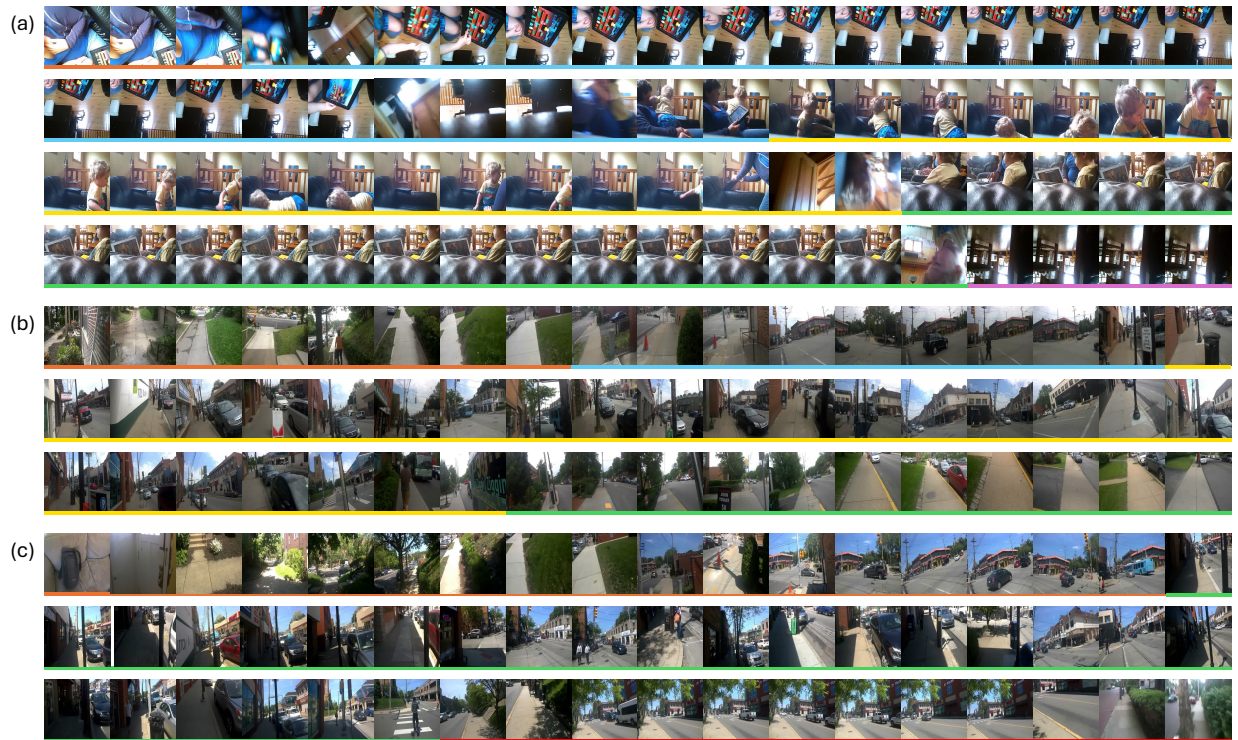


Figure 8: **Visualization of the temporal segments produced by randomly initialized models on (a) SAYCam (b)(c) KrishnaCam.** The images are the same as the ones in Figure 3. We observe that Memory Storyboard training enables to model to capture more intricate transitions between scenes.